Bioorg. Med. Chem. 36 (2021) 116044

Contents lists available at ScienceDirect

Bioorganic & Medicinal Chemistry

journal homepage: www.elsevier.com/locate/bmc

The natural-based optimization of kojic acid conjugated to different thio-quinazolinones as potential anti-melanogenesis agents with tyrosinase inhibitory activity

Nima Sepehri [a], Aida Iraji [b,c], Ali Yavari [d], Mohammad Sadegh Asgari [e], Saeed Zamani [f], Samanesadat Hosseini [g], Saeed Bahadorikhalili [d], Somayeh Pirhadi [b], Bagher Larijani [d], Mahsima Khoshneviszadeh [b], Halleh Hamedifar [h], Mohammad Mahdavi [d,*], Mehdi Khoshneviszadeh [b,f,*]

[a] Nano Alvand Company, Avicenna Tech Park, Tehran University of Medical Sciences, Tehran, Iran
[b] Medicinal and Natural Products Chemistry Research Center, Shiraz University of Medical Sciences, Shiraz, Iran
[c] Central Research laboratory, Shiraz University of Medical Sciences, Shiraz, Iran
[d] Endocrinology and Metabolism Research Center, Endocrinology and Metabolism Clinical Sciences Institute, Tehran University of Medical Sciences, Tehran, Iran
[e] School of Chemistry, College of Science, University of Tehran, Tehran, Iran
[f] Department of Medicinal Chemistry, Faculty of Pharmacy, Shiraz University of Medical Sciences, Shiraz, Iran
[g] Shahid Beheshti University of Medical Sciences, Tehran, Iran
[h] CinnaGen Medical Biotechnology Research Center, Alborz University of Medical Sciences, Karaj, Iran

ARTICLE INFO

Keywords:
Tyrosinase inhibitor
Hyperpigmentation
Kojic acid
Quinazolinone
Cytotoxicity

ABSTRACT

Melanin pigment and melanogenesis are a two-edged sword. Melanin has a radioprotection role while melanogenesis has undesirable effects. Targeting the melanogenesis pathway, a series of kojyl thioether conjugated to different quinazolinone derivatives were designed, synthesized, and evaluated for their inhibitory activity against mushroom tyrosinase. All the synthesized compounds were screened for their anti-tyrosinase activity and all derivatives displayed better potency than kojic acid as the positive control. In this regard, **5j** and **5h** as the most active compounds showed an IC_{50} value of 0.46 and 0.50 μM, respectively. In kinetic evaluation against tyrosinase, **5j** depicted an uncompetitive inhibition pattern. Designed compounds also exhibited mild antioxidant capacity. Moreover, **5j** and **5h** achieved good potency against the B16F10 cell line to reduce the melanin content, whilst showing limited toxicity against malignant cells. The proposed binding mode of new inhibitors evaluated through molecular docking was consistent with the results of structure–activity relationship analysis.

1. Introduction

Melanin is a natural biopolymer widely distributed in many organisms and has important roles ranging from radio to immunoprotection as well as detoxification of chemicals[1]. However, the accumulation of an abnormal amount of melanin pigments in different parts of the skin resulting in melanogenesis known as over synthesis of melanin pigments. Melanogenesis can enhance tumor growth or induce tumor progression[23] as well as increase the risk of cancer and Parkinson's disease[4]. Hyperpigmentation in human skin and enzymatic browning in fruits is not desirable. Enzymatic browning in fruit, crops, and fungi is considered to be deleterious to the quality of plant-derived food, which decreases the commercial value of the products[5].

Signaling pathways in melanogenesis confirming the role of tyrosinase enzyme (TYR) in the catalysis process. In detail, TYR involves two critical reactions: the hydroxylation of monophenols to o-diphenols (monophenolase activity) and the oxidation of o-diphenols to o-quinones (diphenolase activity). Finally, o-quinone is transformed into melanin in a series of non-enzymatic reactions[6]. In detail, during the monophenolase activity, deoxy form of tyrosinase (E_{deoxy} containing

* Corresponding authors at: Endocrinology and Metabolism Clinical Sciences Institute, Tehran University of Medical Sciences, Tehran, Iran (M. Mahdavi). Medicinal and Natural Products Chemistry Research Center, Shiraz University of Medical Sciences, Shiraz, Iran. Department of Medicinal Chemistry, Faculty of Pharmacy, Shiraz University of Medical Sciences, Shiraz, Iran (M. Khoshneviszadeh).
E-mail addresses: momahdavi@sina.tums.ac.ir (M. Mahdavi), khoshnevim@sums.ac.ir (M. Khoshneviszadeh).

https://doi.org/10.1016/j.bmc.2021.116044
Received 20 October 2020; Received in revised form 9 January 2021; Accepted 20 January 2021
Available online 27 January 2021

Cu^{+}) binds to oxygen and form oxy-tyrosinase (E_{oxy} containing Cu^{2+}). Next E_{oxy} binds to L-tyrosine and catalyzed it to L-Dopa. In the diphenolase cycle, both the E_{oxy} and E_{met} forms react with o-diphenol, oxidizing it to the o-quinone[7].

As a result, TYR inhibitors have gained high attention in the therapies of skin pathologies and as well as in dermo-cosmetic treatments and central nervous system (CNS) disorders. Due to the increasing demand for TYR inhibitors, a large number of natural, (including phenolic, chalcones, flavanone, resveratrol, cinnamic acid derivatives), and synthetic inhibitors (phenyl-derived, thiourea, indole, thiosemicarbazide) have been developed over the past few years[8–10]. Common TYR inhibitors suffer from toxicity and lack of efficacy[11]. As a result, new potent TYR inhibitors to use are hot topic nowadays[7].

Also, UV irradiation can produce reactive oxygen species (ROS) and reactive nitrogen species (RNS) which upregulate melanogenesis by activating TYR. These reactive species enhance the damage of DNA and may induce the proliferation of melanocytes. Therefore ROS scavengers such as antioxidants may reduce hyperpigmentation.

2. Results and discussion

2.1. Designing consideration

Kojic acid (**A**) is known as a powerful anti-TYR due to its capacity to reduce back o-dopaquinone to L-Dopa and avoiding melanin formation. Also, kojic acid demonstrated a promising antioxidant capacity with photoprotective, anti-inflammatory, and pain-relieving actions[12]. However, kojic acid has some adverse effects as it is known as an irritating agent with high cytotoxicity and instability in storage[13]. To improve its stability, absorption, and hypopigmented effect, different structural modifications on kojic acid were performed[14]. In this regard, series of kojyl thioether were designed and synthesized. Compound **B** exhibited moderate anti-TYR activity with IC_{50} = 23.95 μM with no cytotoxicity up to 100 μM. The IC_{50} value of kojic acid as a positive control against TYR was 89.41 μM. Also, compound **B** effectively inhibited NO production *via* the suppression of iNOS mRNA expression[15]. In the other study, modification on kojic acid resulted in kojyl thioether derivatives with IC_{50} value ranging from 0.087 to 79.87 μM which were more active than the standard inhibitor kojic acid with IC_{50} = 87.38 μM (Compound **C** as the most potent compound was depicted in Fig. 1)[16]. The SAR study showed that the presence of the sulfide linkage is a critical factor to improve TYR inhibitory activity. From a biological viewpoint, it is deduced that sulfur-containing compounds have high potency toward TYR owing to form hydrogen bonding acceptor and chelate transition metals such as copper[17–18].

For the past few years, there are limited reports of quinazolines as a family of TYR inhibitors[19]. In this respect, 2-(4-fluorophenyl)-quinazolin-4(3H)-one (compound **D**) exhibited IC_{50} of 120 ± 2 μM compared to that of arbutin as another standard TYR inhibitor (IC_{50} = 180 μM)[20]. Dige et al. introduced oxoquinazolin-3(4H)-yl)furan-2-carboxamide derivatives (compound **E**) and all of these compounds were found to be potent inhibitors with an IC_{50} value of 0.028 to 1.775 μM[21]. In 2019, compound **F** was identified as another highly potent entry against TYR[22].

It should be noted that an effective TYR inhibitor with antioxidant potential which reducing the melanin content in the cell-based assay, could successfully decrease associated undesirable side effects of melanogenesis. However, the question remains about the toxicity and activity of these compounds in the cell-based assay. As a result, in the present study, the molecular hybridization approach of potent pharmacophore groups was applied to design kojyl thioether linked to quinazolinone derivatives (Fig. 1). These compounds were first evaluated as TYR inhibitors. Next, the most potent derivatives were further evaluated for their toxicity and potential to reduce melanin content on melanoma B16F10 cells. It was assumed that the designed inhibitors offer several advantages. First, the presence of phenols mimicking substrates with copper- chelating potency (kojyl thioether) is the most effective means to inactivate the TYR enzyme. Secondly, promising reducing capacity and antioxidant potential of kojic acid have been showing in various studies in such a way that reduces back o-dopaquinone to L-Dopa, and avoiding melanin formations. Thirdly, kojyl thio-quinazoline due to containing S, OH, and NH groups, making very likely to interact with

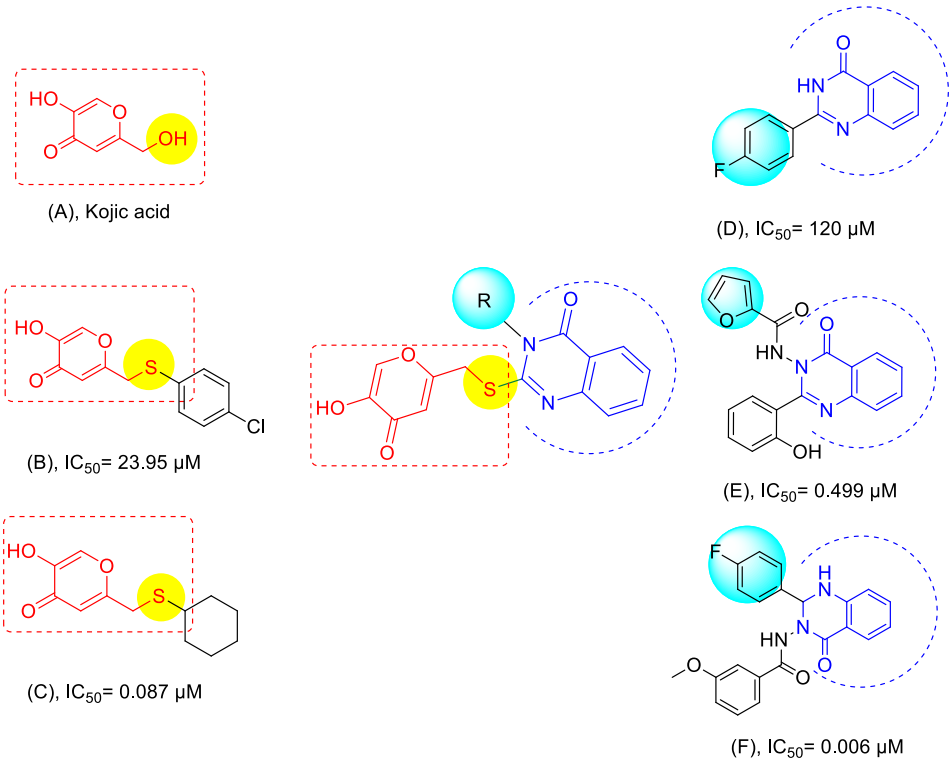

Fig. 1. Designing a series of kojyl thioether based compounds conjugated to different quinazoline derivatives.

copper ions at the TYR active site and also the trapping of o-dopaquinone (precursors to form colorless conjugates). Derivatization of the hybridized backbone was performed on quinazolinone *via* the involvement of different aryl pendants with effective antioxidant and radical scavenging potential.

2.2. Chemistry

In an attempt to provide the structural features for TYR inhibitory activity, a series of kojic acid conjugated to different quinazolinone derivatives were synthesized according to the previously reported method[23]. The synthetic pathway is depicted in scheme 1.

First, commercially available isatoic anhydride (**1**) was reacted with different amine (**2**) in refluxing ethanol for 3 h, then carbon disulfide (1 mmol) in EtOH was added to the mixture to afford compound **3**. Compound **5a-o** was synthesized through nucleophilic substitution reaction of commercially available kojyl chloride (**4**) with compound **3** in DMF and a catalytic amount of K_2CO_3 to the afforded final product. The crude product was purified by recrystallization in ethanol. The structures of purified products were confirmed by IR, ^{1}H NMR, ^{13}C NMR, and mass spectroscopy.

2.3. Evaluation of TYR inhibitory activity and structure–activity relationship

The TYR inhibitory activity of 15 derivatives of kojic acid linked to different quinazolinone scaffold was determined based on the colorimetric method against mushroom tyrosinase comparing with kojic acid as the reference drug. Each experiment was performed three to five times for all compounds and the mean percent of inhibition of TYR enzymatic activity was calculated at the different concentrations. The results are summarized in Table 1.

The obtained results revealed that most of the compounds showed significant inhibition against TYR at the concentrations of 10 μM (ranging from 71.72 to 98.79% inhibition) and 0.5 μM (ranging from 11.39 to 54.48% inhibition).

In particular, **5j** was the most promising TYR inhibitor of this series (IC_{50} = 0.46 μM) with around 20 times increase in the activity compared to kojic acid as positive control possibly owing to the presence of methylpyridine moiety at the R position. The other potent compound in this series was **5h** (IC_{50} = 0.50 μM) and **5e** (IC_{50} = 0.50 μM). Based on our results and considering the substituted quinazolinones structure–activity relationship (SAR) was constructed for the designed scaffold.

2.3.1. Assessment of substituted group at R position

- The effects of substituted groups on phenyl derivatives (**5a-f**) indicated that compounds **5a** (unsubstantiated moiety**)** showed an IC_{50} value of 1.88 μM.
- From the screening data, the presence of the electron-donating group had negative effects on TYR inhibitory activity. In detail, methylation of the phenyl group resulted in a significant reduction of TYR inhibitory potential compared to the unsubstantiated one (**5b**, IC_{50} = 5.32 μM). Although the presence of methoxy as a bulk-electron donating group (**5c**) led to an improvement of TYR inhibitory activity comparing with methyl-substituted one (**5b**), the inhibitory potency did not improve compared to an unsubstantiated moiety. Multi-methoxy substitutions on phenyl ring (**5d**) did not show significant differences compared to **5c**. On the other hand, comparison of electron-donating groups demonstrated that an increase in hydrophilicity has more positive roles in the anti-TYR activity. In this regard compounds, **5c** and **5d** showed better inhibition activity compared to **5b** with a methyl group.
- In the case of compounds containing an electron-withdrawing group, it can be seen that **5e** (R = *para*-Cl, IC_{50} = 0.50 μM) and **5f** (R = *para*-Br, IC_{50} = 1.48 μM) demonstrated superior TYR inhibitory potential than their phenyl counterpart **5a** and even positive control. The order of activity in halogen substitution can be considered as the following order Cl > Br which could be due to moderate lipophilicity and/or moderate bulkiness of Cl-containing derivative compare to Br counterpart.
- Pyridine derivative **5h** (IC_{50} = 0.5 μM) also demonstrated significant inhibitory potential compared with the un-substituted counterpart **5a**.
- It was worth noting that although compound **5g** exerted a moderate inhibition activity (IC_{50} = 2.1 μM) compared to the rest of the tested compounds, it still had approximately 4 fold better activity than the positive control.

2.3.2. Assessment of methyl-substituted group at R position

At first look, it can be seen that elongation of the alkyl linker between the quinazolinone and R pendants may result in improved TYR inhibitory potential in most cases. This is obvious in the compounds **5i** (R = benzyl) with an IC_{50} value of 1.42 μM and **5j** (R = methylpyridine) with an IC_{50} value of 0.46 μM compare to **5a** (IC_{50} value of 1.88 μM) and **5 h** (R = pyridine, IC_{50} = 0.5 μM) counterparts.

2.3.3. Assessment of aliphatic substituted pendant

In this group, the top potent TYR inhibitor belonged to **5m** (R =

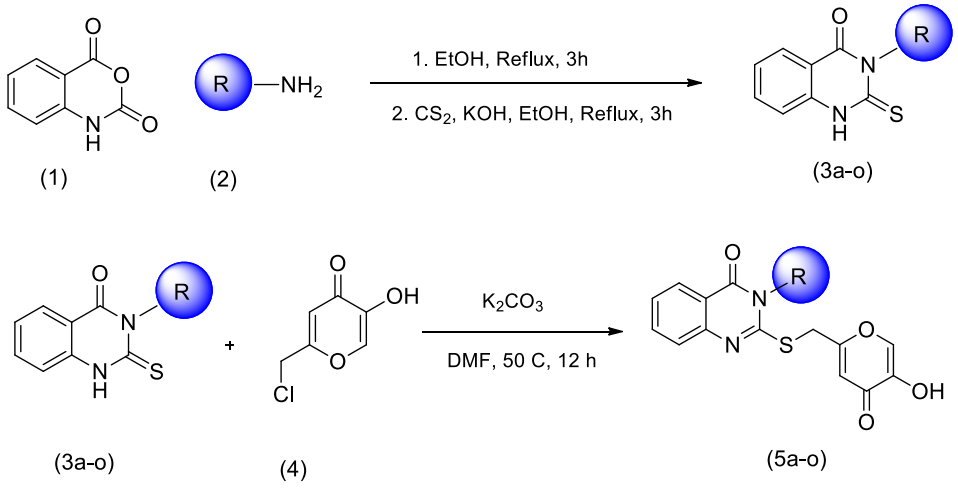

Scheme 1. Synthesis pathway for the preparation of kojic acid linked to different thio-quinazolinone derivatives.

Table 1
The anti-TYR activity of kojic acid linked to different quinazolinone **5a-o**[a] in the presence of L-Dopa.

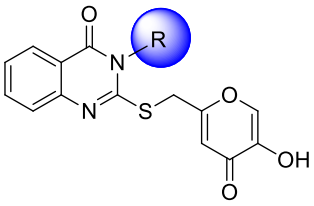

Compounds		Tyrosinase inhibition			DPPH assay
Entry	R	% Inhibition at 10 μM (±SE) [a]	% Inhibition at 0.5 μM (±SE) [a]	IC_{50} μM (±SE) [a]	% Inhibition at 100 μM (±SE) [c]
5a	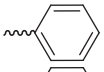	91.68 (±5.33)	42.99 (±4.18)	1.88 (±0.24)	31.43 (±4.55)
5b	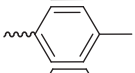	77.32 (±3.84)	11.39 (±5.27)	5.32 (±1.56)	33.30 (±2.64)
5c	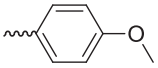	83.52 (±2.14)	22.12(±6.39)	2.40 (±0.76)	27.14 (±4.76)
5d	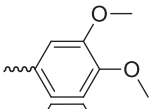	98.79 (±6.57)	40.12 (±4.81)	2.12 (±0.84)	24.52 (±2.78)
5e	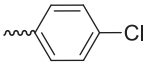	94.25 (±4.87)	49.49 (±6.47)	0.50 (±0.05)	32.62 (±1.74)
5f	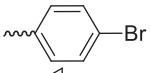	71.72 (±3.59)	40.12 (±5.11)	1.48 (±0.71)	33.34 (±3.66)
5 g		82.46 (±5.17)	23.64 (±7.12)	2.10 (±0.89)	24.52 (±5.74)
5 h	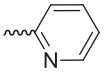	90.93 (±3.68)	50.55 (±3.41)	0.50 (±0.02)	33.81 (±3.77)
5i	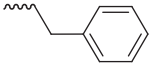	94.10 (±4.81)	42.54 (±5.86)	1.42 (±0.11)	27.86 (±5.11)
5j	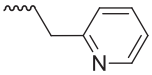	90.32 (±3.11)	54.48 (±2.63)	0.46 (±0.90)	42.56 (±3.62)
5 k	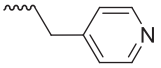	88.51 (±6.27)	15.93 (±4.27)	2.2 (±0.84)	39.05 (±4.26)
5 l	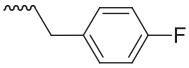	91.98 (±5.93)	32.40 (±5.69)	1.56 (±0.41)	32.62 (±5.19)
5 m		91.22 (±4.79)	38.61(±4.52)	1.44 (±0.71)	32.62 (±6.98)
5n	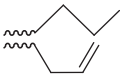	90.47 (±6.52)	24.54 (±6.37)	2.31 (±0.88)	22.62 (±5.44)
5o		91.98 (±4.83)	32.40 (±4.72)	1.56 (±0.61)	ND
Kojic Acid [b]				9.30 (±1.27)	
Quercetin [d]					4.62 (±2.26)

[a] Data presented here are the mean ± S.E.M. of three to six independent experiments.
[b] Used as a positive control.
[c] The values represent mean ± S.E.M (n = 3–5).
[d] Quercetin was used as a standard positive control agent.

isopropyl) with an IC_{50} value of 1.44 μM followed by **5o** (R = propyl, IC_{50} = 1.56 μM) and **5n** (R = butene, IC_{50} = 1.56 μM). However, it seems that this structural modification did not demonstrate significant improvement in the TYR inhibitory potency.

2.4. Kinetic studies

Kinetic studies were conducted to examine the mechanism of inhibition by compound **5j** towards TYR. The obtained values for the K_m and V_m are summarized in Table 2. Graphical analysis of the reciprocal Lineweaver–Burk plot related to compound **5j** described an uncompetitive inhibition pattern against TYR (Fig. 2 and Table. 2) indicating that

Table 2
Kinetic parameters for the compounds **5j** against mushroom tyrosinase inhibition assay.

Compound	K_m (mM)	V_m (OD/Min)
5j (0 μM)	37.31	8.92
5j (0.5 μM)	1.68	0.27
5j (2.5 μM)	1.149	0.15
5j (10 μM)	0.92	0.081

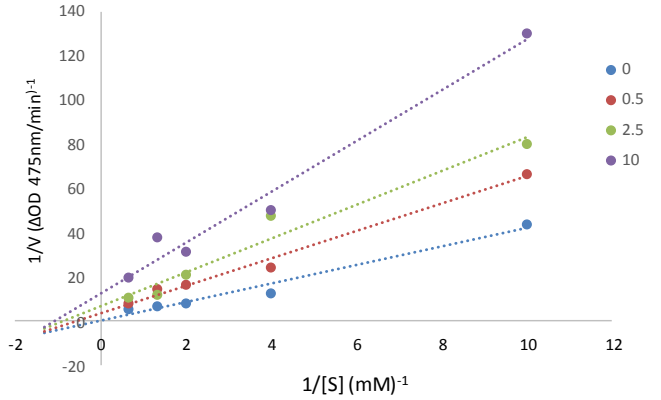

Fig. 2. Lineweaver–Burk plot for the inhibition of mushroom tyrosinase-catalyzed L-Dopa oxidation by **5j.**

5j binds to the complex formed between the enzyme and the substrate.

2.5. Antioxidant activity

Antioxidant-rich diets have shown a significant correlation between free radical-scavenging and tyrosinase-inhibiting activities. In other words, ROS scavengers such as antioxidants may reduce hyperpigmentation. Therefore, in addition to TYR inhibition, the antioxidant activity of the targeted compounds may additionally alleviate symptoms of monogenesis. To this end, the antioxidant activity of the synthesized compounds was also evaluated and presented in Table 1.

Interestingly, compounds bearing a pyridine pendant demonstrated superior radical scavenging potential compared to other derivatives. The order of antioxidant activity was **5j (R** = 2-methylpyridine > **5k** (R = 4-methylpyridine) > **5h** (R = 2-pyridine). It is maybe due to their ability to donate an electron, decline oxidative stress and eliminate ROS and RNS[24]. Replacement of the pyridine substituted with electron-donating groups (compound **5b, 5c,** and **5d**) resulted in a decrease in antioxidant activity. Also, the compounds bearing aliphatic moieties **5o** (R = butane, % Inhibition at 100 μM = not detect), and **5n** (R = propyl, % Inhibition at 100 μM = 22.62) demonstrated week antioxidant potential compared to other (hetero)aromatic derivatives.

2.6. Molecular docking simulation and validation of docking

To further elucidate the possible binding mechanism of potent compounds with the TYR active site, molecular docking using Autodock 4.2 was performed. The structure of the TYR inhibitor was obtained from the PDB data bank (PDB code: 2Y9X). The top-ranked docking score of the inhibitor was superimposed over the X-ray coordinates of the experimentally derived structure. The docked and actual inhibitor structures were superimposed with an RMSD of 1.8 Å (RMSD < 2 Å is the acceptable value). Considering the results of the molecular docking study, the following results were obtained.

Docking binding energy of Compound **5h** was −10.88 kcal/mol. As depicted in Fig. 3, C═O of pyran-4-one ring was fixed within TYR active site through two H-bonds interaction with critical His259 and His85 coordinated with CuA and CuB. Another H-bound interaction was seen between O of pyran-4-one and His263. Also, the pyran-4-one moiety of compound **5h** demonstrated π interactions *via* His263, Ser282, Val283, and Ala286. Pyridine ring was involved in π-π interactions with Val283 and Ala286. On the other hand, the quinazolinone pendant was captured by Val248 and Phe264 *via* π-π and π-alkyl interactions. Also, thioether linker formed a hydrogen bond with Val283. Mentioned results confirming the high potency of **5h**

The interactions of the best-docked confirmation of **5j** with the active site residues of 2Y9X are depicted in Fig. 4. This compound recorded −11.14 kcal/mol value as binding energy. Similar to **5h**, C═O of pyran-4-one ring showed two important H-bonds interactions with critical His61 and His263. Also, pyran-4-one moiety participates in π-π stacking and π-aryl interactions with His263, and Ala286. O of pyran-4-one increases energy minimizing in the active site through hydrogen bond interaction linked with CuA which justifies the high potency of these derivatives. Whilst at the opposite side, the quinazolinone part of **5j** showed π-π T-shape and π-π stacking interactions with Phe264 and Pro277 as well as π-alkyl interaction with Val248. Terminal methyl-

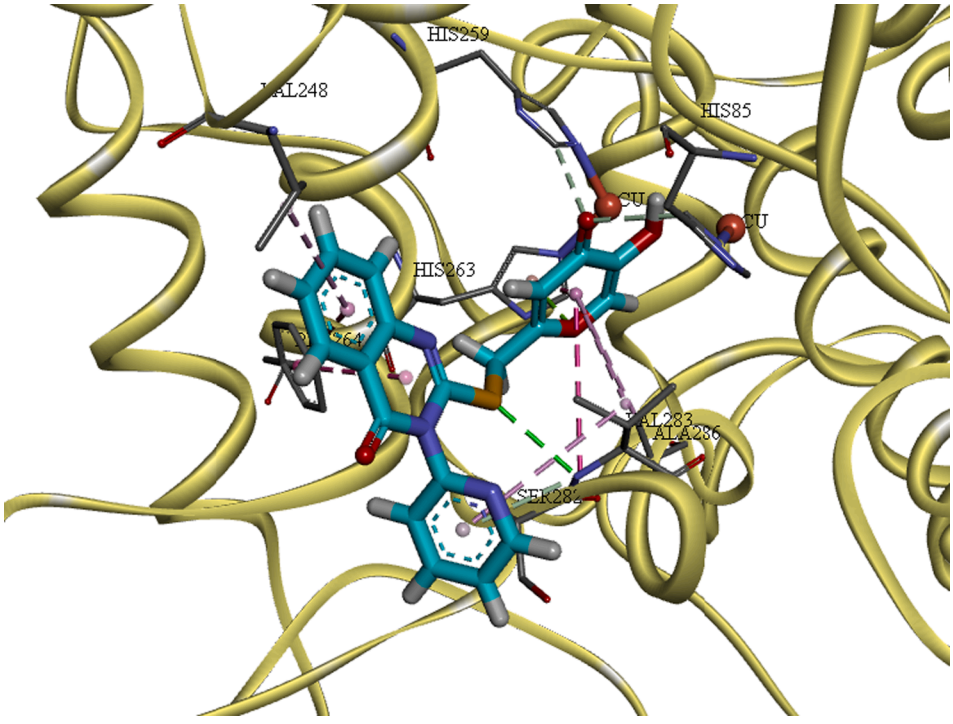

Fig. 3. Compound **5h** was docked to the binding pocket of the 2Y9X.

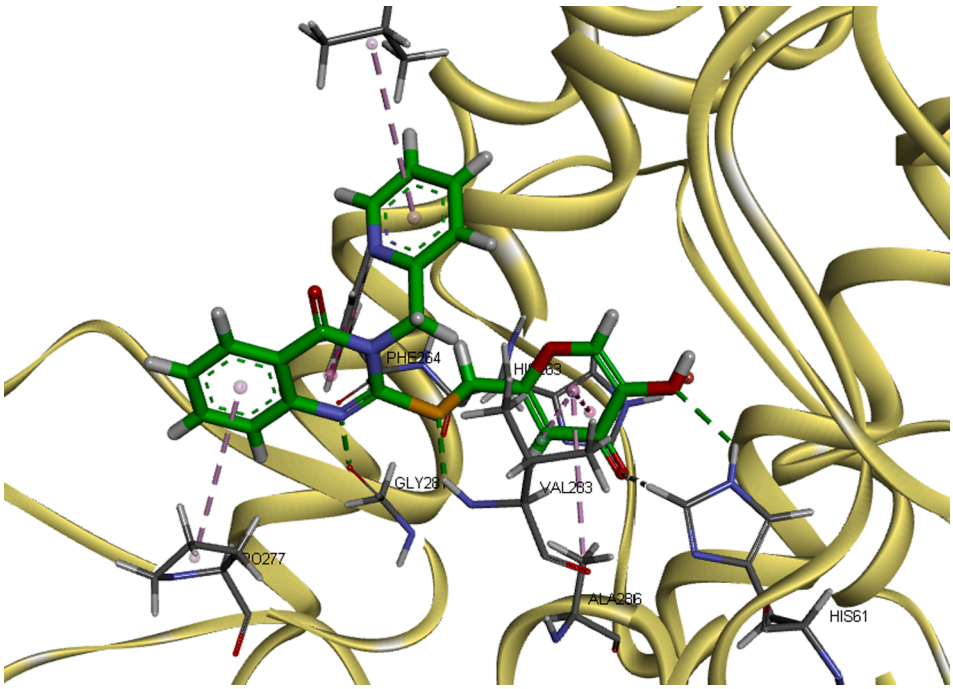

Fig. 4. Compound **5j** was docked to the binding pocket of the 2Y9X.

pyridine was involved in π-aryl interactions with Val248. This potent compound also showed hydrogen bond interaction between thioether linker and Val283.

Figure 5 represented binding interactions of compound **5k** (moderately active compound) over 2Y9X. This derivative exhibited binding energies of −9.04 kcal/mol. The targeted compound produced conventional H-bonding interaction with His85 *via* O of pyran-4-one moiety. The mentioned ring also depicted van der Wals and π-π T-shape interactions with His63. Also, two π-aryl interactions were seen between pyran-4-one moiety and Ala286 and Val283. The methyl-pyridine group made a π-π T-shaped and π-aryl interactions with His244 and Val283. Quinazolinone made a π-π stacked interaction with Phe264. In this derivative, the thiourea group did not participate in any interactions.

Taken together, the molecular interaction studies suggested that interaction with at least one His residue linked to Cu cofactor is essential for the primary improvement of TYR inhibition which justifies moderate to the high potency of these compounds. Further molecular docking investigation revealed that additional H-bond interactions with thioether as seen in **5h** and **5j** improve ligand-enzyme interaction and potency.

2.7. Cell viability

5h and **5j** showed the best tyrosinase inhibitory activity as well as scavenging capacity, so its ability to affect the viability of invasive melanoma B16F10 cell line was also evaluated. B16F10 cells were

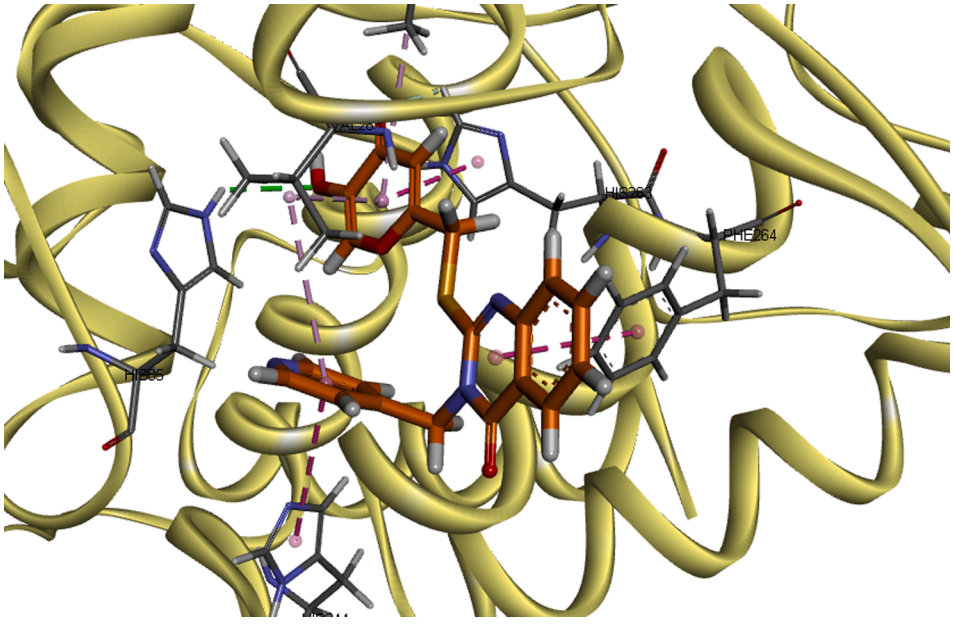

Fig. 5. Compound **5k** was docked to the binding pocket of the 2Y9X.

treated with the mentioned compounds at different concentrations using the MTT test. Compounds **5h** and **5j** did not show any toxicity at 2 and 4 μM (Table 3) and moderate to low toxic effect at 8 μM. Yet, the anti-TYR IC_{50s} of compound **5h** and **5j** were 0.5 and 0.45 μM respectively, it seems that both compounds could be served as potential anti-melanogenesis lead in the non-toxic concentrations for further investigation.

2.8. Melanin content assay

The idea behind anti-melanogenesis lies in the hypothesis that monophenolase and diphenolase activity of TYR contributes to the activation of melanogenesis and potent TYR inhibitors should reduce melanin content. As a result, the effect of the most potent TYR inhibitors was tested on the melanin production of B16F10 melanoma cells. The percentages of melanin content for **5h** and **5j** are presented as mean ± SD compared to the negative control group (untreated) and positive control group (kojic acid, 100 μM). As can be seen in Fig. 6, both compounds reduced the melanin content in skin melanoma cells even at 2 μM concentration compared to kojic acid at 100 μM. More specifically, the best potency was seen in **5j** which demonstrated 68.99% melanin content at 8 μM so fewer than that of kojic acid at 100 μM with 94.24% melanin content. The same pattern with fewer effects was seen in compound **5h** depicted 75.05% melanin content at 8 μM.

3. Conclusion

Structure-based optimization was conducted to improve the inhibitory potency of synthesized compounds against TYR compared to kojic acid. In this regard, kojic thioether moiety conjugated with quinazolinones were designed and synthesized. All compounds did exhibit promising anti-TYR activity so that **5h** and **5j** showed around 20-fold increased in potency compared to the literature compound against TYR. *In vitro,* kinetic evaluation of **5j** showed uncompetitive type inhibition. Anti-melanogenesis of the mentioned compounds was further supported by the reduction in melanin content on B16F10 melanoma cells that was better than the positive control. These compounds were further evaluated for their toxicities on B16F10 cells (MTT assay). Molecular docking studies highlighted the important interactions of selected conjugated kojic thioether derivatives in the active site of TYR *via* H bound interactions with His residues.

Thus, kojyl thioether conjugated to different quinazolines as effective and safe TYR inhibitors with the potential to reduce melanin content can be considered as therapeutics agents worthy of further investigation.

4. Material and method

4.1. Chemistry

Isatoic anhydride (compound **1**, 1 mmol) was dissolved in ethanol (20 ml), different amines (compound **2**, 1.1 mmol) were added and the mixture was refluxed for about 3 h. Then the carbon disulfide (1 mmol) and a catalytic amount of KOH were added to the mixture to afford compounds **3a-o**. After completion of the reaction (monitored by TLC), the precipitate was filtered and recrystallized in EtOH. Next, commercially available kojyl chloride (**4**), different thioxo-2,3-dihydroquinazolin-4(1H)-one derivative (**3a-o),** and a catalytic amount of K_2CO_3 was dissolved in DMF. The reaction mixture was then stirred at 50 °C for 12 h to the afforded final product.

Table 3
Toxicity of the most potent test compounds against B16F10 cells examined by MTT assay.

Compound	Cell viability (%) 2 μM	4 μM	8 μM
5 h	97.87 ± 9.87	91.15 ± 10.43	60.51 ± 10.41
5j	94.21 ± 10.86	83.48 ± 12.30	63.11 ± 1025

Presented data are the mean (±S.E.M.) of three to six independent determinations.

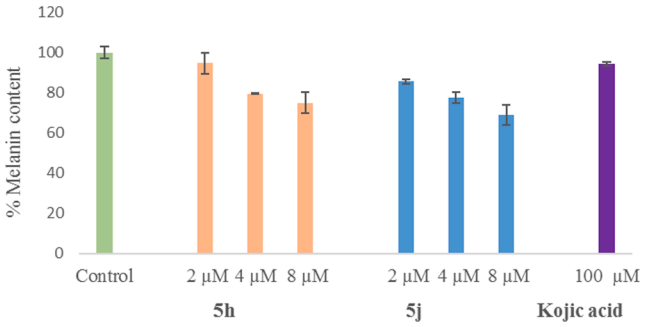

Fig. 6. Effect of compounds **5j** and **5h** on melanin content in the B16F10 cell line.

4.1.1. 2-(((5-hydroxy-4-oxo-4H-pyran-2-yl)methyl)thio)-3-phenylquinazolin-4(3H)-one (5a)

White solid; isolated yield: 94%; mp 159–161 °C; IR (KBr, υ): 3490, 3057, 1639, 1095 cm^{-1}; ^1H NMR (500 MHz, DMSO-d_6) δ 9.35 (s, 1H, OH), 8.20 (d, J = 6.7 Hz, 1H), 8.14 (d, J = 7.7 Hz, 1H), 7.83 (t, J = 7.5 Hz, 1H), 7.72 (d, J = 7.8 Hz, 1H), 7.55 (d, J = 10.5 Hz, 1H), 7.50 (t, J = 7.4 Hz, 1H), 7.23 (d, J = 8.2 Hz, 1H), 7.15 (d, J = 7.4 Hz, 2H), 5.38 (s, 1H, H_b), 5.31 (s, 1H, H_a), 4.93 (s, 2H, S-CH_2); ^{13}C NMR (126 MHz, DMSO-d_6) δ 184.4, 162.7, 160.2, 152.2, 142.6, 138.2, 135.0, 132.2, 129.8, 127.8, 126.6, 126.3, 121.6, 115.3, 115.2, 79.0, 26.1; Anal Calcd for $C_{20}H_{14}N_2O_4$, C, 63.48; H, 3.73; N, 7.40 found: C, 63.51; H, 3.77; N, 7.47.

4.1.2. 2-(((5-hydroxy-4-oxo-4H-pyran-2-yl)methyl)thio)-3-(p-tolyl) quinazolin-4(3H)-one (5b)

White solid; isolated yield: 79%; mp 203–205 °C; IR (KBr, υ): 3491, 3054, 1637, 1091 cm^{-1}; ^1H NMR (500 MHz, DMSO-d_6) δ 8.88 (s, 1H, OH), 7.72 (d, J = 8.1 Hz, 1H), 7.50 (t, J = 7.3 Hz, 1H), 7.35 (t, J = 7.0 Hz, 2H), 7.30 (d, J = 8.4 Hz, 2H), 7.22 (d, J = 8.3 Hz, 2H), 5.28 (s, 1H, H_b), 5.21 (s, 1H, H_a), 4.33 (s, 2H, S-CH_2), 2.21 (s, 3H, CH_3); ^{13}C NMR (126 MHz, DMSO-d_6) δ 165.83, 161.12, 159.73, 157.24, 142.50, 134.97, 129.97, 129.91, 129.84, 128.81, 127.84, 127.75, 127.45, 126.75, 126.59, 126.28, 115.19, 30.44, 19.26; Anal Calcd for $C_{21}H_{16}N_2O_4$, C, 64.27; H, 4.11; N, 7.14 found: C, 64.24; H, 4.16; N, 7.09.

4.1.3. 2-(((5-hydroxy-4-oxo-4H-pyran-2-yl)methyl)thio)-3-(4-methoxyphenyl)quinazolin-4(3H)-one (5c)

White solid; isolated yield: 91%; mp 189–191 °C; IR (KBr, υ): 3498, 3051, 1631, 1097 cm^{-1}; ^1H NMR (500 MHz, DMSO-d_6) δ 9.58 (s, 1H, OH), 8.20 (d, J = 7.5 Hz, 2H), 8.14 (d, J = 7.8 Hz, 1H), 7.82 (t, J = 7.5 Hz, 1H), 7.72 (d, J = 8.0 Hz, 1H), 7.50 (t, J = 6.8 Hz, 1H), 7.15 (d, J = 8.2 Hz, 2H), 5.39 (s, 1H, H_b), 5.31 (s, 1H, H_a), 4.93 (s, 2H, S-CH_2), 4.04 (s, 3H, OCH_3); ^{13}C NMR (126 MHz, DMSO-d_6) δ 182.8, 179.8, 175.6, 170.9, 165.6, 160.2, 135.0, 129.9, 127.7, 126. 9, 126.6, 126.3, 126.0, 122.1, 121.2, 115.2, 79.0, 56.1, 29.3; Anal Calcd for $C_{21}H_{16}N_2O_5$, C, 61.76; H, 3.95; N, 6.86 found: C, 61.70; H, 3.91; N 6.85.

4.1.4. 3-(3,4-dimethoxyphenyl)-2-(((5-hydroxy-4-oxo-4H-pyran-2-yl) methyl)thio)quinazolin-4(3H)-one (5d)

White solid; isolated yield: 84%; mp 227–229 °C; IR (KBr, υ): 3488, 3050, 1641, 1096 cm^{-1}; ^1H NMR (500 MHz, DMSO-d_6) δ 9.41 (s, 1H, OH), 8.32 (s, 1H), 8.22 – 8.20 (m, 1H), 8.14 (d, J = 7.8 Hz, 1H), 7.83 (t, J = 7.0 Hz, 1H), 7.43 (d, J = 8.4 Hz, 1H), 7.38 (t, J = 8.0 Hz, 1H), 7.08 (d, J = 7.6 Hz, 1H), 5.50 (s, 1H, H_b), 5.30 (s, 1H, H_a), 4.08 (s, 2H, S-CH_2), 3.85 (s, 3H, OCH_3), 3.82 (s, 3H, OCH_3); ^{13}C NMR (126 MHz, DMSO-d_6) δ 181.8, 165.5, 162.7, 161.1, 136.6, 135.0, 132.5, 129.9, 128.6, 127.8,

127.6, 126.9, 126.6, 126.6, 126.3, 124.9, 115.2, 114.9, 52.4, 26.6; Anal Calcd for $C_{22}H_{18}N_2O_4$, C, 60.27; H, 4.14; N, 6.39 found: C, 60.33; H, 4.17; N, 6.37.

4.1.5. 3-(4-chlorophenyl)-2-(((5-hydroxy-4-oxo-4H-pyran-2-yl)methyl) thio)quinazolin-4(3H)-one (5e)

White solid; isolated yield: 89%; mp 175–177 °C; IR (KBr, υ): 3492, 3051, 1635, 1092 cm^{-1}; ^1H NMR (500 MHz, DMSO-d_6) δ 9.61 (s, 1H, OH), 8.00 (d, $J = 8.2$ Hz, 1H), 7.83 (s, 1H), 7.72 (d, $J = 9.1$ Hz, 2H), 7.49 (d, $J = 7.7$ Hz, 1H), 7.43 (t, $J = 7.9$ Hz, 1H), 7.25 – 7.20 (m, 2H), 5.49 – 5.44 (m, 1H, H_b), 5.30 (d, $J = 2.5$ Hz, 1H, H_a), 4.03 (d, $J = 7.2$ Hz, 2H, S-CH_2); ^{13}C NMR (126 MHz, DMSO-d_6) δ 183.0, 163.5, 157.0, 156.9, 150.4, 141.6, 138.9, 135.0, 134.6, 129.9, 129.9, 126.3, 126.0, 125.52, 115.2, 110.4, 77.5, 31.7; Anal Calcd for $C_{20}H_{13}N_2O_4$, C, 58.18; H, 3.17; N, 6.79 found: C, 58.17; H, 3.11; N, 6.82.

4.1.6. 3-(4-bromophenyl)-2-(((5-hydroxy-4-oxo-4H-pyran-2-yl)methyl) thio)quinazolin-4(3H)-one (5f)

White solid; isolated yield: 93%; mp 182–184 °C; IR (KBr, υ): 3489, 3051, 1639, 1090 cm^{-1}; ^1H NMR (500 MHz, DMSO-d_6) δ 9.49 (d, $J =$ 5.1 Hz, 1H, OH), 7.83 (t, $J = 8.4$ Hz, 1H), 7.72 (d, $J = 7.7$ Hz, 1H), 7.61 (d, $J = 7.5$ Hz, 1H), 7.43 (d, $J = 8.3$ Hz, 2H), 7.08 (d, $J = 7.4$ Hz, 2H), 7.03 (s, 1H), 5.31 (s, 1H, H_b), 5.18 (s, 1H, H_a), 4.09 (s, 2H, S-CH_2); ^{13}C NMR (126 MHz, DMSO-d_6) δ 185.1, 164.0, 158.8, 156.0, 142.9, 133.7, 131.9, 130.2, 129.9, 128.7, 127. 8, 126.6, 121.3, 117.5, 115.2, 114.8, 114.5, 29.8; Anal Calcd for $C_{20}H_{13}N_2O_4$, C, 52.53; H, 2.87; N, 6.13 found: C, 52.49; H, 2.85; N, 6.11.

4.1.7. 3-cyclopropyl-2-(((5-hydroxy-4-oxo-4H-pyran-2-yl)methyl)thio) quinazolin-4(3H)-one (5 g)

White solid; isolated yield: 92%; mp 171–174 °C; IR (KBr, υ): 3499, 3055, 1631, 1097 cm^{-1}; ^1H NMR (500 MHz, DMSO-d_6) δ 9.67 (s, 1H, OH), 7.82 (d, $J = 8.0$ Hz, 1H), 7.72 (d, $J = 8.0$ Hz, 1H), 7.50 (t, $J = 7.3$ Hz, 1H), 7.23 (d, $J = 9.2$ Hz, 1H), 5.47 (s, 1H, H_b), 5.31 (s, 1H, H_a), 4.12 – 4.01 (m, 3H), 1.47 – 1.29 (m, 2H, CH_2-Cyclopropyl), 1.13 – 1.04 (m, 2H, CH_2-Cyclopropyl); ^{13}C NMR (126 MHz, DMSO-d_6) δ 185.0, 163.8, 160.1, 152.4, 142.0, 135.0, 129.8, 127.8, 126. 7, 126.3, 121.2, 119.5, 115.3, 32.2, 30.0, 8.6; Anal Calcd for $C_{17}H_{14}N_2O_4$, C, 59.64; H, 4.12; N, 8.18 found: C, 59.61; H, 4.06; N, 8.12.

4.1.8. 2-(((5-hydroxy-4-oxo-4H-pyran-2-yl)methyl)thio)-3-(pyridin-2-yl) quinazolin-4(3H)-one (5 h)

White solid; isolated yield: 89%; mp 206–208 °C; IR (KBr, υ): 3488, 3055, 1639, 1099 cm^{-1}; ^1H NMR (500 MHz, DMSO-d_6) δ 10.09 (s, 1H, OH), 8.31 (s, 1H), 8.21 (d, $J = 7.8$ Hz, 2H), 8.14 (d, $J = 7.4$ Hz, 1H), 7.83 (t, $J = 7.6$ Hz, 1H), 7.72 (d, $J = 7.6$ Hz, 1H), 7.50 (t, $J = 7.4$ Hz, 1H), 7.38 (d, $J = 7.7$ Hz, 1H), 5.44 (s, 1H, H_b), 5.30 (s, 1H, H_a), 3.99 (s, 2H, S-CH_2); ^{13}C NMR (126 MHz, DMSO-d_6) δ 183.4, 169.1, 162.5, 158.3, 148.0, 143.5, 139.9, 135.0, 129.9, 127.4, 122.4, 115.2, 109.1, 105.6, 100.6, 79.4, 33.0; Anal Calcd for $C_{19}H_{13}N_3O_4$, C, 60.15; H, 3.45; N, 11.08 found: C, 60.11; H, 3.50; N, 11.05.

4.1.9. 3-benzyl-2-(((5-hydroxy-4-oxo-4H-pyran-2-yl)methyl)thio) quinazolin-4(3H)-one (5i)

White solid; isolated yield: 82%; mp 177–179 °C; IR (KBr, υ): 3492, 3051, 1639, 1094 cm^{-1}; ^1H NMR (500 MHz, DMSO-d_6) δ 9.21 (s, 1H, OH), 7.74 (d, $J = 9.3$ Hz, 1H), 7.61 (d, $J = 7.5$ Hz, 1H), 7.54 (d, $J = 8.0$ Hz, 1H), 7.43 (d, $J = 7.0$ Hz, 1H), 7.35 (t, $J = 7.5$ Hz, 1H), 7.23 (d, $J =$ 6.7 Hz, 2H), 7.08 (d, $J = 7.2$ Hz, 1H), 7.02 (s, 1H), 5.71 (s, 1H, H_b), 5.46 (s, 1H, H_a), 5.18 (s, 2H, N-CH_2), 4.04 (s,2H, S-CH_2); ^{13}C NMR (126 MHz, DMSO-d_6) δ 182.9, 158.7, 154.3, 148.4, 133.7, 130.1, 129.9, 128.6, 128.0, 127.8, 127.2, 126.7, 126.3, 117.5, 115.4, 115.2, 114.8, 52.4, 30.3; Anal Calcd for $C_{21}H_{16}N_2O_4$, C, 64.27; H, 4.11; N, 7.14 found: C, 64.25; H, 4.14; N, 7.08.

4.1.10. 2-(((5-hydroxy-4-oxo-4H-pyran-2-yl)methyl)thio)-3-(pyridin-2-ylmethyl)quinazolin-4(3H)-one (5j)

White solid; isolated yield: 85%; mp 193–195 °C; IR (KBr, υ): 3492, 3053, 1641, 1095 cm^{-1}; ^1H NMR (500 MHz, DMSO-d_6) δ 9.31 (s, 1H, OH), 8.33 (s, 1H), 8.21 (d, $J = 7.2$ Hz, 2H), 8.14 (d, $J = 7.6$ Hz, 1H), 7.83 (t, $J = 6.3$ Hz, 1H), 7.76 (d, $J = 7.7$ Hz, 1H), 7.50 (t, $J = 6.9$ Hz, 1H), 7.44 (d, $J = 8.3$ Hz, 1H), 5.48 (s, 1H, H_b), 5.31 (s, 1H, H_a), 4.93 (s, 2H, N-CH_2), 4.03 (s, 2H, S-CH_2); ^{13}C NMR (126 MHz, DMSO-d_6) δ 184.0, 165.4, 162.7, 161.1, 155.3, 151.4, 149.4, 142.4, 137.7, 135.0, 130.2, 129.91, 127.8, 127.3, 121.6, 115.2, 81.1, 52.3, 27.3; Anal Calcd for $C_{20}H_{15}N_3O_4$, C, 61.06; H, 3.84; N, 10.68 found: C, 61.01; H, 3.85; N, 10.72.

4.1.11. 2-(((5-hydroxy-4-oxo-4H-pyran-2-yl)methyl)thio)-3-(pyridin-4-ylmethyl)quinazolin-4(3H)-one (5 k)

White solid; isolated yield: 78%; mp 231–234 °C; IR (KBr, υ): 3488, 3058, 1647, 1087 cm^{-1}; ^1H NMR (500 MHz, DMSO-d_6) δ 9.11 (s, 2H, OH), 8.29 (s, 1H), 8.21 (d, $J = 7.1$ Hz, 2H), 8.14 (d, $J = 5.2$ Hz, 1H), 7.83 (t, $J = 7.4$ Hz, 1H), 7.72 (d, $J = 8.9$ Hz, 1H), 7.61 (d, $J = 7.7$ Hz, 1H), 7.50 (t, $J = 7.4$ Hz, 1H), 5.29 (s, 1H, H_b), 5.17 (s, 1H, H_a), 4.93 (s, 2H, N-CH_2), 4.10 (s, 2H, S-CH_2); ^{13}C NMR (126 MHz, DMSO-d_6) δ 186.6, 172.3, 168.7, 161.6, 155.6, 151.1, 140.3, 130.8, 130.5, 129.9, 128.6, 127.78, 124.2, 119.5, 114.8, 76.4, 47.0, 29.1; Anal Calcd for $C_{20}H_{15}N_3O_4$, C, 61.06; H, 3.84; N, 10.68 found: C, 61.03; H, 3.78; N, 10.62.

4.1.12. 2-(((5-hydroxy-4-oxo-4H-pyran-2-yl)methyl)thio)-3-isopropylquinazolin-4(3H)-one (5 m)

White solid; isolated yield: 86%; mp 187–189 °C; IR (KBr, υ): 3492, 3058, 1633, 1096 cm^{-1}; ^1H NMR (500 MHz, DMSO-d_6) δ 9.58 (s, 1H, OH), 7.83 (t, $J = 7.5$ Hz, 1H), 7.72 (d, $J = 8.3$ Hz, 1H), 7.61 (d, $J = 7.7$ Hz, 1H), 7.52 – 7.47 (m, 1H), 5.71 (s, 1H, H_b), 5.44 (s, 1H, H_a), 5.20 – 5.15 (m, 1H, CH), 4.93 (s, 2H, S-CH_2), 1.21–1.15 (m, 6H); ^{13}C NMR (126 MHz, DMSO-d_6) δ 177.9, 164. 9, 158.8, 154.9, 135.0, 133.7, 129.9, 129.1, 128.6, 126.7, 126.3, 117.5, 115.3, 114.8, 51.8, 32.0, 22.3; Anal Calcd for $C_{17}H_{16}N_2O_4$, C, 59.29; H, 4.68; N, 8.13 found: C, 59.32; H, 4.72; N, 8.10.

4.1.13. 2-(((6-hydroxy-4-oxo-4H-pyran-2-yl)methyl)thio)-3-propylquinazolin-4(3H)-one (5n)

White solid; isolated yield: 96%; mp 212–214 °C; IR (KBr, υ): 3485, 3049, 1638, 1096 cm^{-1}; ^1H NMR (500 MHz, DMSO-d_6) δ 9.89 (s, 1H, OH), 8.14 (d, $J = 8.0$ Hz, 0H), 7.83 (t, $J = 7.8$ Hz, 0H), 7.72 (d, $J = 8.1$ Hz, 0H), 7.50 (t, $J = 7.7$ Hz, 0H), 5.38 (s, 1H, H_b), 5.30 (s, 1H, H_a), 4.42 (s, 2H, N-CH_2), 4.03 (t, $J = 3.4$ Hz, 2H, S-CH_2), 1.83 (h, $J = 3.0$ Hz, 2H, CH_2), 1.06 (t, $J = 7.8$ Hz, 3H, CH_3); ^{13}C NMR (126 MHz, DMSO-d_6) δ 164.8, 162.7, 161.1, 152.3, 149.4, 142.6, 137.8, 135.0, 129.3, 126.9, 121.3, 115.2, 33.3, 26.4, 16.7, 7.3; Anal Calcd for $C_{17}H_{16}N_2O_4$, C, 59.29; H, 4.68; N, 8.13 found: C, 59.22; H, 4.71; N, 8.18.

4.1.14. 3-allyl-2-(((5-hydroxy-4-oxo-4H-pyran-2-yl)methyl)thio) quinazolin-4(3H)-one (5o)

White solid; isolated yield: 88%; mp 235–237 °C; IR (KBr, υ): 3485, 3053, 1639, 1098 cm^{-1}; ^1H NMR (500 MHz, DMSO-d_6) δ 8.88 (s, 1H, OH), 7.83 (t, $J = 6.6$ Hz, 1H), 7.72 (d, $J = 7.8$ Hz, 1H), 7.50 (t, $J = 7.4$ Hz, 1H), 7.21 (s, 1H), 5.38 (d, $J = 13.8$ Hz, 2H, C = CH_2), 5.28 (s, 1H, H_a), 5.21 – 5.16 (m, 2H, N-CH_2), 4.87 (d, $J = 5.6$ Hz, 2H), 4.32 (s, 2H, S-CH_2); ^{13}C NMR (126 MHz, DMSO-d_6) δ 181.4, 163.3, 153.7, 139.7, 135.0, 129.9, 129.9, 129.8, 124.2, 122.7, 120.9, 115.6, 115.4, 115.2, 52.1, 31.2; Anal Calcd for $C_{17}H_{14}N_2O_4$, C, 59.64; H, 4.12; N, 8.18 found: C, 59.62; H, 4.19; N, 8.14.

4.2. TYR enzymatic assay

Stock solutions of all derivatives were prepared in DMSO. At first 160 μL of phosphate buffer (50 mM, pH = 6.8) was added to 10 μL tyrosinase (5771 units/mg solid, 0.5 mg/mL) in separate wells of a black 96-well microplate and afterward, 10 μL of inhibitors were added and

gently mixed. Then the plate was shaken for 20 min and 20 μL of L-Dopa was added to each well to start the reaction. Upon the addition of L-Dopa, the absorbance was read immediately for 10 min in 475 nm. Experiments were repeated three to five times and the mean percent of enzyme inhibitory activities at 0.1, 0.5, 1, 10, 50 and 100 μM concentrations of test compounds were calculated. CurveExpert software version 1.34 for Windows was used to calculate IC_{50} values from the concentration–inhibition curves.

4.3. Kinetic characterization of TYR inhibition

To obtain the mechanism of action of compound **5j**, reciprocal plots of 1/velocity versus 1/[substrate] were constructed at different concentrations of L-Dopa (0.25, 0.5, 0.75 and 1 mM). as the substrate by colorimetric method. Compound **5j** at different concentrations was added to the assay solution and preincubated with the enzyme at room temperature for 10 min, followed by the addition of the substrate. Preincubation and measurement time was the same as discussed in the mushroom tyrosinase inhibition assay protocol. Kinetic measurement catalyzed by enzyme was conducted at 475 nm. The inhibition type of the enzyme was assayed by Line weaver Burk plots of the inverse of velocities (1/V) versus the inverse of substrate concentrations 1/[S] mM.

4.4. Determination of the reducing activity of the stable radical DPPH

The free radical-scavenging capacity of the synthesized compounds was tested by the DPPH method. Quercetin was used as positive control and methanol as the negative control. Briefly, 180 μL of a methanolic solution of DPPH (110 μM) were added to 20 μL of different concentrations of the tested compounds dissolved in DMSO. The mixture was shaken vigorously for 20 min at room temperature in dark. The absorbance was determined spectrophotometrically at 517 nm and the percentage of activity was calculated. All tests were performed on three replicates and the results were compared with the quercetin as standard.

4.5. Determination of melanin content

The effect of targeted compounds on melanin content was studied on B16F10 melanoma cells. The cells were seeded in a 12-well plate overnight in RPMI media supplemented with 10% fetal bovine serum (FBS; Gibco, USA), penicillin (100 units/mL), and streptomycin (0.1 mg/mL). Then tested compounds at different concentrations were added to the cell culture to reach the concentration of 2, 4, and 8 μM. After 24 h, the cells were harvested by trypsin and washed with PBS. The obtained cell pellets were treated with aqueous NaOH (2 M, 100 μL) and incubated at 100 °C for 0.5 h. The absorption of each well was recorded at 405 nm using a Synergy H4 Hybrid Multi-Mode Microplate Reader (BioTek).

4.6. Toxicity assay on B16F10 melanoma cells

The toxic effect of the most potent TYR inhibitor compounds (**5h** and **5j**) was assessed against B16F10 melanoma cells MTT reduction assay. PC12 cells were obtained from Pasture Institute, Iran. Cells were grown at 37 °C in the presence of CO_2 5% in DMEM (Gibco BRL, Grand Island, NY, USA), 10% fetal bovine serum (FBS, Gibco BRL), and penicillin/streptomycin (100 IU/mL and 100 μg/mL, respectively). The cells were cultured into a 96-well plate at a density of 1×10^3 cells/ml (100 μL in each well) and incubated for 48 h to adhere at 37 °C. Synthesized derivatives at various concentrations were added in triplicate to each well and incubated at 37 °C for 24 h in a CO_2 incubator. After incubating, 20 μL of MTT solution (2 mg/mL) was added to each well and incubated for 4 h and then the supernatant was removed. The formazan dye was solubilized by adding 150 μL DMSO to each well, followed by gentle shaking. The optical density was measured at 570 nm using a Bio-Rad microplate reader (Model 680, Bio-Rad). Each experiment was repeated 3–46 times. IC_{50} values were calculated by best-fit equations using the Curve Expert statistical program.

4.7. Docking study

The computer simulation was performed using the molecular docking software, AutoDock 4.2 with the help of Autodock Tools. The structures of the molecules were drawn by Chem3D Ultra 8.0 software, then optimized the molecules to the minimum energy conformation used the semi-empirical MM^+ method. The Gastiger charges and torsional degrees of freedom were assigned on the generated PDB files by ADT 1.5.4. Lamarckian genetic algorithm was employed for this analysis with the following settings: 100 runs for each ligand; 2,500,000 as the maximum number of energy evaluations; 27,000 as the maximum number of generations. The grid box was set with 60, 60, and 60 points in the ×, y, and z directions, respectively, with the default grid spacing of 0.375 Å. All other options were set as default.

Declaration of Competing Interest

The authors declared that there is no competing of interest.

Acknowledgment

The authors wish to thank the support of the Vice-Chancellor for Research of Shiraz University of Medical Sciences (grant number: 98-01-12-20819). This study was part of the Pharm.D thesis of Saeed Zamani.

Appendix A. Supplementary data

Supplementary data to this article can be found online at https://doi.org/10.1016/j.bmc.2021.116044.

References

1 Smith DF, Casadevall A. The role of melanin in fungal pathogenesis for animal hosts. *Fungal Physiology Immunopathogenesis*. 2019:1–30.
2 Slominski RM, Zmijewski MA, Slominski AT. The role of melanin pigment in melanoma. *Exp Dermatol*. 2015;24:258–259.
3 Kim YJ, Kang KS, Yokozawa T. The anti-melanogenic effect of pycnogenol by its anti-oxidative actions. *Food Chem Toxicol*. 2008;46:2466–2471.
4 Bose A, Petsko GA, Eliezer D. Parkinson's disease and melanoma: co-occurrence and mechanisms. *J Parkinson's disease*. 2018;8:385–398.
5 Iraji A, Adelpour T, Edraki N, Khoshneviszadeh M, Miri R, Khoshneviszadeh M. Synthesis, biological evaluation and molecular docking analysis of vanilline-benzylidenehydrazine hybrids as potent tyrosinase inhibitors. *BMC chemistry*. 2020;14:28.
6 Buitrago E, Hardre R, Haudecoeur R, et al. Are human tyrosinase and related proteins suitable targets for melanoma therapy? *Curr Top Med Chem*. 2016;16:3033–3047.
7 Pillaiyar T, Namasivayam V, Manickam M, Jung S-H. Inhibitors of melanogenesis: an updated review. *J Med Chem*. 2018;61:7395–7418.
8 Zolghadri S, Bahrami A, Hassan Khan MT, et al. A comprehensive review on tyrosinase inhibitors. *J Enzyme Inhib Med Chem*. 2019;34:279–309.
9 Lee SY, Baek N, Nam T-G. Natural, semisynthetic and synthetic tyrosinase inhibitors. *J Enzyme Inhib Med Chem*. 2016;31:1–13.
10 A. Iraji, Z. Panahi, N. Edraki, M. Khoshneviszadeh, M. Khoshneviszadeh, Design, synthesis, in vitro and in silico studies of novel Schiff base derivatives of 2-hydroxy-4-methoxybenzamide as tyrosinase inhibitors, Drug Development Research, n/a.
11 Kumari S, Thng STG, Verma NK, Gautam HK. Melanogenesis inhibitors. *Acta dermato-venereologica*. 2018;98:924–931.
12 Monteiro RC, Kishore BN, Bhat RM, Sukumar D, Martis J, Ganesh HK. A Comparative Study of the Efficacy of 4% Hydroquinone vs 0.75% Kojic Acid Cream in the Treatment of Facial Melasma. *Indian J Dermatol*. 2013;58:157.
13 Noh J-M, Kwak S-Y, Kim D-H, Lee Y-S. Kojic acid–tripeptide amide as a new tyrosinase inhibitor. *Pept Sci*. 2007;88:300–307.
14 Cho J-C, Rho HS, Baek HS, et al. Depigmenting activity of new kojic acid derivative obtained as a side product in the synthesis of cinnamate of kojic acid. *Bioorg Med Chem Lett*. 2012;22:2004–2007.
15 Rho H-S, Yoo D-S, Ahn S-M, Kim M-K, Cho D-H, Cho J-Y. Inhibitory activities of kojyl thioether derivatives against nitric oxide production induced by lipopolysaccharide. *Bull Korean Chem Soc*. 2010;31:3463–3466.
16 Rho HS, Ahn SM, Yoo DS, Kim MK, Cho DH, Cho JY. Kojyl thioether derivatives having both tyrosinase inhibitory and anti-inflammatory properties. *Bioorg Med Chem Lett*. 2010;20:6569–6571.

17 Francuski BM, Novaković SB, Bogdanović GA. Electronic features and hydrogen bonding capacity of the sulfur acceptor in thioureido-based compounds. Experimental charge density study of 4-methyl-3-thiosemicarbazide. *CrystEngComm*. 2011;13:3580–3591.
18 Vortisch V, Kroneck P, Hemmerich P. Model studies on the coordination of copper in enzymes. IV. Structure and stability of cuprous complexes with sulfur-containing ligands. *J Am Chem Soc*. 1976;98:2821–2826.
19 Li Q, Yang H, Mo J, et al. Identification by shape-based virtual screening and evaluation of new tyrosinase inhibitors. *PeerJ*. 2018;6, e4206.
20 Wang R, Chai W-M, Yang Q, Wei M-K, Peng Y. 2-(4-Fluorophenyl)-quinazolin-4(3H)-one as a novel tyrosinase inhibitor: Synthesis, inhibitory activity, and mechanism. *Bioorg Med Chem*. 2016;24:4620–4625.
21 Dige NC, Mahajan PG, Raza H, et al. Ultrasound mediated efficient synthesis of new 4-oxoquinazolin-3(4H)-yl)furan-2-carboxamides as potent tyrosinase inhibitors: Mechanistic approach through chemoinformatics and molecular docking studies. *Bioorg Chem*. 2019;92, 103201.
22 Mahajan PG, Dige NC, Vanjare BD, et al. Facile synthesis of new quinazolinone benzamides as potent tyrosinase inhibitors: Comparative spectroscopic and molecular docking studies. *J Mol Struct*. 2019;1198, 126915.
23 Asadi M, Masoomi S, Ebrahimi SM, et al. Convenient and sequential one-pot route for synthesis of 2-thioxoquinazolinone and quinazolinobenzothiazinedione derivatives. *Monatshefte Chemie-Chemical Monthly*. 2014;145:497–504.
24 Fubini B, Hubbard A. Reactive oxygen species (ROS) and reactive nitrogen species (RNS) generation by silica in inflammation and fibrosis. *Free Radical Biol Med*. 2003; 34:1507–1516.